Proceedings of the 8th WSEAS International Conference on APPLIED MATHEMATICS, Tenerife, Spain, December 16-18, 2005 (pp25-30)

Numerical solution of a singularly perturbed two-point boundary-value problem using collocation

M. F. PATRÍCIO
University of Coimbra
Department of Mathematics
Apartado 3008, 3001-454 Coimbra
PORTUGAL

P. M. ROSA
Instituto Superior de Engenharia de Coimbra
Department of Physics and Mathematics
Rua Pedro Nunes, 3030-199 Coimbra
PORTUGAL

Abstract: In this paper we study a class of numerical methods to solve a singularly perturbed two-point boundary value problem. Our schemes arise as result of choosing an appropriate basis for the solution, as well as making use of collocation. It is possible to obtain arbitrarily high-order methods. We note that, in some cases (constant coefficients), we obtain the exact solution. Particular attention is paid to time-independent problems, being time-dependent problems also included.

Key–Words: Boundary-value problems, finite differences, nonuniform grids, collocation.

1 Introduction

Consider the singularly perturbed problem (SPP)

$$\begin{cases} Lu := -\epsilon u'' + b(x)u' + c(x)u = f(x), \\ \quad u(0) = u(1) = 0, \quad x \in]0,1[, \end{cases} \tag{1}$$

with $b(x) > 0$, $c(x) \geq 0$, $0 < \epsilon \ll 1$ and $f(x) \geq 0$.

It is well known that the boundary layer for this problem is close to $x = 1$.

Solutions of singularly perturbed boundary-value problems change abruptly in layers. Consequently, discretization methods based on equidistant meshes have difficulty in representing these solutions, in particular when we associate central or upwind differences to those meshes.

A useful approach for solving problem (1) is to consider nonuniform meshes together with finite-differences. Within these types of meshes we can refer piecewise-uniform meshes (for example, Shishkin meshes [14] and Bakhvalov meshes [2]). Other authors propose meshes that are built adaptatively by equidistributing a monitor function (see, for example, [3], [4], [7] and [13]).

For problem (1) with $b(x) = f(x) = 1$ and $c(x) = 0$, we determined the numerical solution using an uniform grid (with step-size h), and with a Shishkin nonuniform mesh. In both cases, the derivatives were discretized using central differences. For different values of parameter ϵ, we present in table 1 the error – ℓ_2 – of the obtained solution.

A brief comparison between the 3rd and 4th columns of table 1 allows us to conclude that the use of a nonuniform Shishkin mesh produces more accurate results (for the same corresponding values of h and ϵ) than the ones obtained with an uniform mesh. Notice, however, that this procedure, although quite accurate, has a high computational cost.

Table 1: Errors (ℓ_2) obtained by central finite differences.

ϵ	h	Uniform mesh	Shishkin mesh
10^{-2}	10^{-1}	9.195×10^{-1}	1.022×10^{-1}
	10^{-2}	4.457×10^{-2}	1.626×10^{-3}
	10^{-3}	1.319×10^{-3}	6.638×10^{-5}
10^{-3}	10^{-1}	1.020×10^{1}	1.373×10^{-1}
	10^{-2}	8.945×10^{-1}	1.423×10^{-2}
	10^{-3}	4.457×10^{-2}	1.505×10^{-4}
10^{-4}	10^{-1}	1.107×10^{2}	1.411×10^{-1}
	10^{-2}	3.536	8.395×10^{-2}
	10^{-3}	8.945×10^{-1}	1.424×10^{-3}
	10^{-4}	4.457×10^{-2}	1.403×10^{-5}

At it is known, (see [6]), the set

$$B = \{\Phi_i, \Psi_i, i = 0, \dots p\}, \quad p \in \mathbb{N}, \tag{2}$$

is a basis for the solution subspace of equation (1), where $\Phi_i(x) = x^i$, $\Psi_i(x) = x^i e^{\frac{1}{\epsilon}g(x)}$ $(i = 0, \dots, p)$, and $g(x) = \int_1^x b(s)\,ds$.

In this work we will use some elements of (2) to approximate the solution of equation (1).

Section 2 will be dedicated to the computation of the discrete solution. Some particular attention will be paid to the case where $c(x) = 0$ and $b(x) = b$ (constant) for all $x \in [0, 1]$.

In section 3 we study the error of the approximation. For such purpose, we will use the residual of the obtained solution. In many cases we obtain the exact solution, and in the other cases a arbitrarily high-precision solution can be obtained.

The procedure presented in section 2 will be extended to time-dependent problems in section 4, time integration being made using a suitable method. Stability behavior is also studied.

We present, in section 5, some computational aspects and an algorithm. Still in this section, some differential equations will be integrated with the developed methods, and we present some comparisons with some classical methods, namely concerning the error and the computational cost.

2 Discrete Approximation

Consider a uniform grid in $[0, 1]$ generating equally-spaced points x_i such that $x_{i+1} = x_i + h$. Suppose that

$$v(x) = A + Bx + Ce^{\frac{1}{\epsilon}g(x)} \tag{3}$$

is an approximation to the solution of (1) on $[x_{i-1}, x_{i+1}]$. At grid-point x_i, we have $v_i = A + Bx_i + Ce^{\frac{1}{\epsilon}g(x_i)}$. Denote by θ_i^{i+1} the quantity $\int_{x_i}^{x_{i+1}} b(t)\,dt$. We then have $g(x_{i+1}) = g(x_i) + \theta_i^{i+1}$. Using the values of v_{i-1}, v_i and v_{i+1}, we can write

$$C = \frac{1}{D_i}\left[(v_{i+1} - 2v_i + v_{i-1})e^{-\frac{1}{\epsilon}g(x_{i-1})}\right], \tag{4}$$

where $D_i := e^{\frac{1}{\epsilon}\theta_{i-1}^{i+1}} - 2e^{\frac{1}{\epsilon}\theta_{i-1}^{i}} + 1$. Therefore,

$$v_{i+1} - v_{i-1} = 2Bh + Ce^{\frac{1}{\epsilon}g(x_{i-1})}\left(e^{\frac{1}{\epsilon}\theta_{i-1}^{i+1}} - 1\right),$$

and thus

$$B = \frac{1}{2h}\left[(v_{i+1} - v_{i-1}) - Ce^{\frac{1}{\epsilon}g(x_{i-1})}\left(e^{\frac{1}{\epsilon}\theta_{i-1}^{i+1}} - 1\right)\right]. \tag{5}$$

Now, let $b_i = b(x_i)$, $c_i = c(x_i)$ and $f_i = f(x_i)$ for all i. Using the fact that $-\epsilon u'' + b_i u' + c_i u = f_i$, and after some algebraic manipulation, we can write

$$\frac{\sigma_i}{D_i}\delta^2 v_i + \frac{1}{2h}(v_{i+1} - v_{i-1}) + \frac{c_i}{b_i}v_i = \frac{f_i}{b_i}, \tag{6}$$

where $\delta^2 v_i := v_{i+1} - 2v_i + v_{i-1}$ and

$$\sigma_i := \left(\frac{1}{\epsilon} - 1 - \frac{1}{\epsilon}b_i\right)e^{\frac{1}{\epsilon}\theta_{i-1}^{i}} - \frac{1}{2h}\left(e^{\frac{1}{\epsilon}\theta_{i-1}^{i+1}} - 1\right).$$

If we approximate function b by a constant in $[x_{i-1}, x_{i+1})$ (say $\beta_i = b(x^*)$ for some x^*) we have $g(x) = \beta_i(x - 1)$. Repeating the above procedure for equation (1) – note that $b(x)$ is not constant here –, we obtain the method

$$\begin{aligned}&\frac{\rho_i\left(1 - \frac{b_i}{\beta_i}\right)}{e^{\rho_i} - e^{-\rho_i}}\delta^2 v_i + \\ &\frac{b_i}{\beta_i}\left(\frac{1 - e^{\rho_i}}{e^{\rho_i} - e^{-\rho_i}}v_{i-1} + v_i + \frac{e^{-\rho_i} - 1}{e^{\rho_i} - e^{-\rho_i}}v_{i+1}\right) \\ = &\frac{h(e^{\rho_i} - 1)}{b_i(e^{\rho_i} + 1)}f_i,\end{aligned} \tag{7}$$

where $\rho_i := \frac{\beta_i h}{\epsilon}$.

As a particular case, if $b(x)$ is constant over the interval $[x_{i-1}, x_{i+1})$ (say $b(x) = b_i$, $x \in [x_{i-1}, x_{i+1})$), then $\beta_i = b_i$, $\theta_{i-1}^i = b_i h$ and therefore method (6) can be rewritten as

$$\begin{aligned}\frac{1 - e^{\rho_i}}{e^{\rho_i} - e^{-\rho_i}}v_{i-1} + v_i + \frac{e^{-\rho_i} - 1}{e^{\rho_i} - e^{-\rho_i}}v_{i+1} + \\ + \frac{h(e^{\rho_i} - 1)}{b_i(e^{\rho_i} + 1)}c_i v_i = \frac{h(e^{\rho_i} - 1)}{b_i(e^{\rho_i} + 1)}f_i,\end{aligned} \tag{8}$$

where $\rho_i := \frac{b_i h}{\epsilon}$.

We note that equation (8) is the Il'in-Allen-Southwell scheme (see [1]).

3 Error Analysis. Some Properties

In this section we will consider $c(x) \equiv 0$, although analogous results could be established if $c \neq 0$.

3.1 Positivity

In pollution-related problems, for example, it is important to assure that the solutions are positive. Following the approach presented in [11], it is easy to establish this property for method (8):

Theorem 1 *Method (8) applied to problem (1) with $c = 0$ produces a positive solution.*

Proof: It suffices to note that (8) gives origin to a linear system whose matrix can be decomposed in the form $I - T$, where T is tridiagonal. Since $T \geq 0$ and a vector w such that $(I - T)w > 0$ exists, the result is straightforward. ■

3.2 Error

Error analysis will be done using the residual. Let

$$R(x) := Lu(x) - f(x), \tag{9}$$

and denote by e the error (difference between the exact and the approximate solution).

Theorem 2 *Let u be the exact solution of problem (1) and $R1$ and $R2$ the residuals associated with two approximations $w1$ and $w2$, respectively. If $R1(x) > R2(x)$ then $e1(x) > e2(x)$, where $e1(x) = u(x) - w1(x)$ and $e2(x) = u(x) - w2(x)$.*

Proof: *This result follows directly from the fact that $L(e1 - e2) > 0$ and from the maximum principle.* ■

We can also establish the following result, the proof being straightforward.

Theorem 3 *Consider again problem (1). The numerical solution, v, obtained with method (7), produces a residual, R, verifying $R(x_i) = 0$, for all i. Furthermore, if $c(x) \equiv 0$ then, for $\bar{x} \neq x_i$, we have:*

i. $R(\bar{x}) = f(x_i) - f(\bar{x})$ *if b is piecewise constant;*

ii. $R(\bar{x}) = \frac{\delta^2 v_i}{e^{\rho_i} + e^{-\rho_i} - 2} + \left[\frac{1}{\epsilon}(b(\bar{x}) - \beta_i) e^{\frac{1}{\epsilon}\beta_i(\bar{x} - x_i)} - \frac{b(\bar{x})\rho_i}{h}\left(\frac{\beta_i}{b_i} - 1\right)\right] + \frac{b(\bar{x})}{b_i} f_i - f(\bar{x})$, *otherwise.*

4 Time-dependent Problem

4.1 The Method

For time-dependent problems, it is possible to adapt the method we previously obtained using a MOL (method of lines) approach. Consider problem

$$\begin{cases} u_t = -\epsilon u_{xx} - b(x) u_x + f(x), \; x \in]0,1[, \; t \geq 0, \\ u(0,t) = u(1,t) = 0, t \geq 0, \\ u(x,0) = s(x), x \in [0,1]. \end{cases} \tag{10}$$

As it is well known, in the solution of this convection-dominated problem we can clearly distinguish two different types of regions for each t. Therefore, it seems natural to apply an analogous procedure to what has been done in the time-independent problem.

We begin by setting up a temporal grid with points $t_j = kj$, $j = 0, 1, \ldots$. As usual, let $u_j^n \approx u(x_j, t_n)$ and $u_{px}|_j^n \approx \frac{\partial^p u}{\partial x^p}(x_j, t_n)$.

In order to approximate the derivatives of u we use the values of B and C given by (5) and (4), respectively. Obviously, time integration can be done with a classical method, in particular Euler's forward method. Following this approach, we obtain the following method:

$$u_j^{n+1} - u_j^n = k\left(\epsilon \, u_{xx}|_j^n - b(x_j) \, u_x|_j^n + f(x_j)\right), \tag{11}$$

where k is the temporal step-size. Letting $n = 0, 1, \ldots$, we construct the numerical solution of (10).

4.2 Stability Behavior

In order to study the stability of method (11), we replace u_j^n by $\xi^n e^{i\gamma jh}$. We can easily (but tediously) prove that the amplification factor, ξ, is such that

$$|\xi| \leq 1 + k|A(\epsilon, h)|,$$

where $A(\epsilon, h) < c\bar{b}$, with $c > 0$ constant (independent of h and k) and $\bar{b}$ is such that $|\bar{b}| > b(x), \forall x \in [0,1]$.

According to this result, method (11) produces solutions whose errors are bounded.

5 Numerical Experiments

In order to illustrate the behavior of the methods presented in sections 2 and 4, we now present some numerical experiments. Moreover, we present an algorithm that describes the procedure used in both time-dependent and time-independent problems, the main purpose of it being the obtention of highly accurate results, with a rather low computational cost.

5.1 Time-Independent Problem

Consider again problem (1) with $b(x) = f(x) = 1$ and $c(x) = 0$. In table 1 we presented some results obtained with classical approaches for solving this problem. If we integrate the same problem using method (6), we obtain the errors presented in table 2. Note that this method (with h much greater than used before) produces much more accurate results, and the errors presented in this table are (most likely!!!) round-off errors...

Table 2: Errors (ℓ_2) obtained by method (6).

ϵ	$h = 0.2$	$h = 0.1$
10^{-2}	1.2×10^{-16}	2.6×10^{-16}
10^{-3}	1.6×10^{-16}	1.4×10^{-16}
10^{-4}	2.3×10^{-16}	2.1×10^{-16}

The errors in table 2 were obtained using the exact solution.

5.1.1 Problem 1: $b(x) = 1$, $c(x) = 0$, $f(x) = e^{-x}$

Consider once more problem (1) like above, but now with $f(x) = e^{-x}$. If we apply method (6) to solve this equation, we obtain an approximate solution, whose error ($||u(x) - v(x)||_2$) we present in table 3.

Table 3: Errors (ℓ_2) obtained by method (6) for $b(x) = 1$, $c(x) = 0$ and $f(x) = e^{-x}$.

ϵ	$h = 0.2$	$h = 0.1$
10^{-2}	0.05097	0.04180
10^{-3}	0.05620	0.05127
10^{-4}	0.05673	0.05222

We note that, in this case, the exact solution is given by

$$u(x) = \frac{e^{-x}(1 - e^{1/\epsilon}) + e^{x/\epsilon}(1/e - 1) + e^{1/\epsilon} - 1/e}{(1 + \epsilon)(e^{1/\epsilon} - 1)}.$$

5.1.2 Problem 2: $b(x) = x + 1$, $c(x) = 0$, $f(x) = e^{-x}$

Now let $b(x) = x + 1$, $c(x) = 0$ and $f(x) = e^{-x}$ in problem (1). If we consider $\epsilon = 10^{-3}$ and apply method (6) with $h = 0.1$, we can plot the results in figure 1.

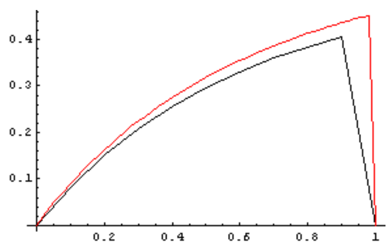

Figure 1: Exact (red) and approximate (black) solutions for problem (1) with $h = 0.1$.

As we can see, the approximation is not acceptable, mainly on $[0.8, 1.0]$. According to theorem 2, we know that associated with a large residual we have a large error. Therefore, we might suspect that over the interval $[0.8, 1.0]$, the residual is large, being zero at $x = 0.9$, according to theorem 3. In fact, if we compute the residual for $x = 0.85$ and 0.95 (the midpoints of sub-intervals $[0.8, 0.9]$ and $[0.9, 1.0]$ respectively) we have $|R(0.85)| \approx 0.0315$ and $|R(0.95)| \approx 0.0305$.

According to there results and, more generally, to theorems 2 and 3, and accepting as a valid criterion that an approximation over an interval $[x_{i-1}, x_{i+1}]$ is unacceptable if the residual at points $x_{i-1/2}$ and $x_{i+1/2}$ exceed a previously established tolerance (say $|R(x_{i\pm1/2})| > \delta$), we can propose the following algorithm: partition the interval $[x_{i-1}, x_{i+1}]$ and apply method (6) on $[x_{i-1}, x_i]$ and $[x_i, x_{i+1}]$, so that the residual at grid-points $x_{i\pm1/2}$ becomes zero. This procedure can be applied to the whole interval $[0, 1]$ or only near the boundary layer.

Returning to the example, if we set $\delta = 0.03$, then the residuals at $x = 0.85$ and $x = 0.95$ are not acceptable. Therefore, we will “refine” the grid on $[0.8, 1]$ and apply again method (6) only on $[0.8, 1]$, but now with $h = \frac{0.1}{2}$. Doing so (which implies that we have accepted the previously computed solution on the interval $[0.0, 0.8]$), we obtain the plots shown in figure 2.

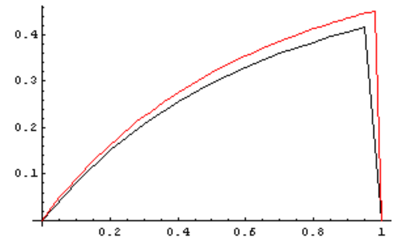

Figure 2: Exact (red) and approximate (black) solutions for problem (1) after refinement on $[0.8, 1.0]$.

The algorithm may be applied again with the purpose of improving the numerical approximation in the boundary layer, or even the approximation all over the interval.

5.2 Time-Dependent Problem

In this subsection we present some numerical results for equation (10) and method (11) with initial data

$$s(x) = \begin{cases} \sin[10\pi(0.5x - 0.1)], & 0.2 < x < 0.4 \\ 0, & \text{otherwise} \end{cases},$$

and two different positive sources. The first one (**problem 1**) is the exponential source $f(x) = \frac{e^{-x}}{2}$, and the second one (**problem 2**) is the discontinuous source

$$f(x) = \begin{cases} 1, & 0.68 < x < 0.80 \\ 0, & \text{otherwise} \end{cases}.$$

In both problems we considered $\epsilon = 10^{-3}$ and $b(x) = 10^{-1}$ for all x. We analise the computational solution for different values of t and compare them with the “exact” solution at the same time-level, obtained with a refined mesh[1]. All results will be presented using the maximum norm, EMAX$= \max_j |u(x_j) - v(x_j)|$.

[1] With $h = \frac{1}{500}$.

5.2.1 Problem 1: Continuous source

In this problem we use $k = \frac{1}{10}$, $h = \frac{1}{40}$ and determine the solution at $t = 1, 5, 10$. In figure 3 we present the "exact" and approximate solutions at $t = 1$ and $t = 10$.

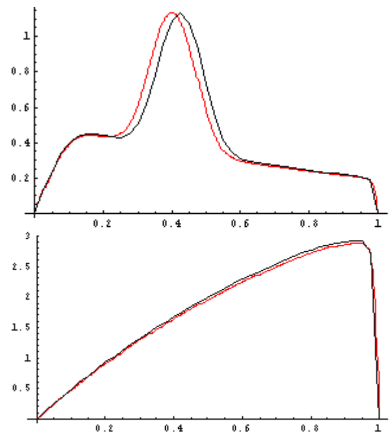

Figure 3: Exact (black) and approximate (red) solutions at $t = 1$ (top) and $t = 10$ (bottom).

For a clearer idea of the errors obtained at different time levels, we present the results in table 4.

Table 4: EMAX errors for problem 1.

	$h = \frac{1}{40}, k = \frac{1}{10}$	$h = \frac{1}{100}, k = \frac{1}{25}$
$t = 1$	0.172	0.071
$t = 5$	0.080	0.043
$t = 10$	0.050	0.027

Some Remarks:

1. Some of these results can be compared with the ones obtained in [12]. Even though the errors are very alike, the computational cost of the method we now present is much lower, namely because we use a fixed mesh, and time integration is done explicitly. We also note that the errors become smaller as time increases.

2. The errors corresponding to $h = \frac{1}{100}$ and $k = \frac{1}{25}$ are included just to obtain a better approximation.

5.2.2 Problem 2: Discontinuous source

In figure 4 (top) we present the approximate and exact solution at $t = 1$ obtained with $h = \frac{1}{40}$ and $k = \frac{1}{10}$, just as it was done in the previous example. We might suspect that the residual is not being controlled, since the error is not acceptable, mainly for $x > 0.2$. It is therefore useful to use the algorithm presented for the time-independent problem in this situation.

In order to control the residual and avoid a high computational cost, we just compute it in some time levels. If the residual is not less than a previously established tolerance (δ), we go back to the previous time level where the residual procedure was successful and recompute the numerical solution with smaller values of h and k (for precision and stability purposes, respectively) only on the region where the test was unsuccessful (large residual). In spatial regions where the test was done successfully, the solution is accepted. After that, we can go on with the same values of h and k, or we can try to increase them.

We note that this procedure is a natural extension of what has been done in section 5.1.

If we use this "algorithm" in this problem, we accept the solution at $t = 1$ for $0 \leq x \leq 0.2$ and refine the mesh for other values of x, using $h = \frac{1}{60}$ and $k = \frac{1}{20}$. In this case these procedure was done going back to $t = 0$ (figure 4 (bottom)).

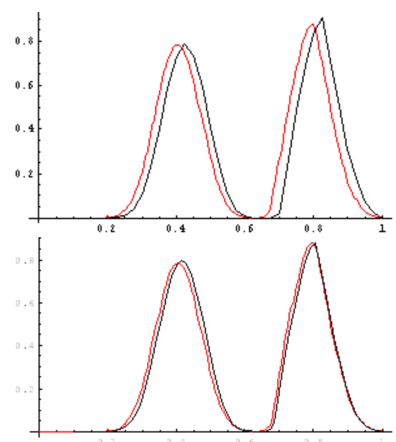

Figure 4: Exact (black) and approximate (red) solutions at $t = 1$.

For values of $t \geq 2$ we tried to increase the values of h and k ($h = \frac{1}{25}$ and $k = \frac{1}{10}$) and computed the approximate solution for $t = 10$ (figure 5).

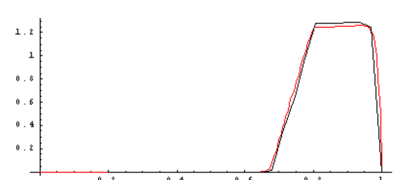

Figure 5: Exact (black) and approximate (red) solutions at $t = 10$.

Some remarks:

– The main advantage of the presented scheme is the fact that it is easy to implement and has a low computational cost.

– Using more elements of (2), we could obtain an arbitrarily high-precision solution. This technique would be similar to the use of extrapolation that was preformed, for example, in [10].

– Apart from the extension to the time-dependent problem, this approach can be adapted to the numerical resolution of sets of singularly perturbed equations. Recently, this problem has been quite researched (see [8] and [9], for example).

Acknowledgements: The authors would like to thank the referees for their helpful suggestions.

References:

[1] Allen, D. N. and Southwell, R. V., *Relaxation methods applied to determine motion, in two dimensions, of a viscous fluid past a fixed cylinder*, Mech. Appl. Math. 8 (1955) 129–145.

[2] Bakhvalov, A. S., *On the optimization of methods for solving boundary value problems with boundary layers*, Zh. Vychisl. Mat. Mat. Fis. 9 (1969) 841–859.

[3] Beckett, G. M., Mackensie, J. A., *Convergence analysis of finite difference approximations on equidistributed grids to a singularly preturbed boundary value problem*, Appl. Numer. Math., 35 (2000), 87–109.

[4] Chen, Y., *Uniform pointwise convergence for a singularly perturbed problem using arc-length equidistribution*, Journal of Computational and Applied Mathematics 159 (2003) 25–34.

[5] Farrell, P. A., O'Riordan, E. and Shishkin, G. I., *A class of singularly preturbed semilinear differential equations with interior layers*, Math. Comp. 74 (2005) 1759–1776.

[6] Gartland, E. C., *Uniform high-order difference schemes for a singularly perturbed two-point boundary-value problem*, J. Math. Comput. 48 (1987) 551–564.

[7] Kopteva, N. K., Madden, N. and Synes, M., *Grid equidistribution for reaction-diffusion problems in one dimension*, Numer. Alorithms 40 (2005) 305–322.

[8] Linß, T., *On a set of singularly preturbed convection-difusion equations*, Journal of Computational and Applied Mathematics, 180, 1 (2005), 173–179.

[9] Madden, N. and Stynes, M., *A uniformly convergent numerical method for a coupled system of two singularly perturbed linear reaction-diffusion problems*, J. Numer. Anal., 23 (2003), 627–644.

[10] Natividad, M. C. and Stynes, M., *Richardson extrapolation for a convection-diffusion problem using a Shishkin mesh*, Appl. Numer. Math., 45 (2003), 315–329.

[11] Oliveira, P. de and Patrício, M. F., *Monotonicity on nonuniform grids*, Journal of Computational and Applied Mathematics, 80 (1997), 171–181.

[12] Oliveira, P. de, Patrício, M. F. and Santos, J., *Positive Solutions with multistep methods for convection-diffusion-reaction equations*, Report number 97–22, Departament of Matemathics, University Coimbra.

[13] Qiu, Y., Sloan, D. M. and Tang, T., *Numerical solution of a singularly perturbed two-point boundary value problem using equidistribution: analysis of convergence*, Journal of Computational and Applied Mathematics, 116 (2000), 121–143.

[14] Shishkin, G. I., *Grid approximation of singularly perturbed elliptic and parabolic equations*, Ph.D. Thesis, Second doctoral thesis, Keldysh Institute of Applied Mathematics, USSR Academy of Science, Moscow, 1990.